Quantitative Analysis of the Impact of Disorder on the Structural and Electrical Properties of Polymer Fibers

R.A. Makin^{1*}, S.N.Hanumantharao², S. Rao^{2,3}, and S.M. Durbin¹
¹Electrical and Computer Engineering, Western Michigan University, Kalamazoo, MI 49008
² Biomedical Engineering, Michigan Technological University, Houghton, MI 49931
³Health Research Institute, Michigan Technological University, Houghton, MI 49931

*robert.makin@wmich.edu

Abstract

Quantifying disorder in physical systems can provide unique opportunities to engineer specific properties. Here, we apply a methodology based on the approach pioneered by Bragg and Williams for metal alloys to quantify the disorder characterizing polymer fibers including polyaniline (PANI), polyaniline-polycaprolactone (PANI-PCL), and polyvinylidene difluoride (PVDF). Both PANI and PVDF possess electrical properties such as conductivity and piezoelectric response, that find a wide range of applications in energy storage and tissue engineering. On the other hand, the mechanical properties of polymer fibers can be tuned by varying the concentration of PANI and PCL during synthesis. Here, we demonstrate that it is possible to control the amount of disorder characterizing a fiber, which provides a route to engineering desired values for specific material properties. The resulting measure of disorder is shown to have a direct relationship to Young's modulus, band gap, and specific capacitance values.

Introduction

Polyaniline (PANI) is one of the most studied polymers due to interest in its electrical conductivity and structural properties [1]. While PANI alone is brittle and shown to be cytotoxic, combining PANI with polycaprolactone results in excellent biocompatibility, as evidenced by extensive reports in the literature in the field of tissue engineering [2]–[6]. Another well-studied polymer is polyvinylidene fluoride (PVDF) due to its piezoelectric properties and its hydrophobic nature which has led to widespread use of PVDF fibers as filters [7]. In this paper, we investigate the impact of disorder on the electrical properties of PANI fibers, and the structural properties of polyaniline-polycaprolactone (PANI-PCL) fibers and PVDF.

It is well-known that disorder exists in physical systems, and that it can be correlated to specific properties. While it is common to approach such an endeavor in a qualitative fashion, employing a quantitative measure of disorder can enable numerical predictions regarding property values, determine their full experimentally-accessible range, and in some cases enable real-time production control during material synthesis. In polymers, disorder is often described or closely tied to the degree of crystallinity, with samples classified on a scale ranging from crystalline to amorphous [8], [9]. Here, we present a methodology—orthogonal to the current approaches—that explores a different facet of disorder in polymers, where even samples with no discernable crystallinity (such as amorphous samples) have a measurable non-zero order parameter. Previously, we demonstrated a methodology for measuring disorder in polypropylene fibers [10] based in part on the pioneering work of Bragg and Williams in the 1930s [11], in which they defined an order parameter S which ranges in value between zero (completely disordered structure) to unity (ordered structure). For such a system, the disorder characterizing individual fibers can be understood on a molecular level in the context of the tacticity of the polymer chains.

Materials and Methods

All the materials were used as procured unless specified. Polycaprolactone (PCL): (MW = 70,000 GPC; Scientific Polymer Products, USA) and Polyaniline (PANI): Emeraldine base (MW = 50,000; Aldrich Chemistry, USA) were used for making the nanostructures. The doped form of PANI-PCL solution was prepared by dissolving equal concentrations of 0.35%wt. emeraldine base and 10-camphorsulfonic acid (CSA) (Aldrich Chemistry; France), and 15% PCL in chloroform (Sigma Aldrich, USA) and filtering the solution using a syringe filter (0.22 μm). The concentration of PANI in the filtered solution was determined post-filtration using UV–vis spectrophotometer (LAMBDA 35; PerkinElmer, Inc). For electrospinning, the voltage was varied between 18 and 24 kV in steps of 1 kV to obtain different nanostructures using a rotating cylinder (EM-DIG and EM-RTC; IME Technologies, Netherlands) as collector. The environmental conditions were maintained as a constant. The tip-collector distance was maintained constant at 0.17 m. For the PCL scaffolds, the parameters used for electrospinning are reported in the previous work [12].

The order parameter of fibers analyzed in this manuscript was measured either from Raman spectra or scanning electron microscopy (SEM) images; examples for both techniques are shown in Figure 1 and follow the methodology described previously [10], [13], [14]. We note that for these techniques a value for S^2 is directly obtained from the measurements, and S can be obtained by then taking the square root.

For Raman spectra, the order parameter can be measured using two peaks, one due to the ordered structure of the fiber and one due to the disordered structure. Following along the framework developed by Loveluck and Sokoloff [15], it can be shown [16] that

$$S^2 = \frac{1}{\frac{J_{S=0}}{J_{S=1}} - 1} \tag{1}$$

where $J_{S=1}$ is the area under the peak associated with the ordered structure and $J_{S=0}$ is the area under the peak associated with the disordered structure. Figure 1a shows the results of S^2 analysis on a Raman spectrum of a PANI sample taken from the literature [17]. The two features are typically identified iteratively using a set of samples having a range of S values; the area under a Raman peak associated with the ordered structure will vary as S^2 , whereas a $(1 - S^2)$ variation characterizes peaks associated with the disordered structure [13], [14].

The S^2 value of a sample can be measured from an SEM image through a contrast analysis technique using the pixel intensity histogram of the image [10], [14]. The analysis fits two curves to the pixel intensity histogram, one representing intensities due to the disordered regions and one representing intensities due to ordered regions of the sample. The ordered structure peak will have a higher central intensity than the other peak, since electrons from ordered regions interfere constructively while electrons from disordered regions interfere destructively. Based on these two fits, a threshold value is chosen at an integer multiple of the standard deviation away from the center of the ordered structure peak, based on relative location of the intersection between the ordered and disordered structure curves [10]. This threshold value is used to separate ordered and disordered component contributions to the image; the S^2 value of the sample is simply the ratio of the total area of ordered structure regions in the image to the total area of the image. Figure 1b shows an example of this analysis applied to an SEM image of a representative PCL sample.

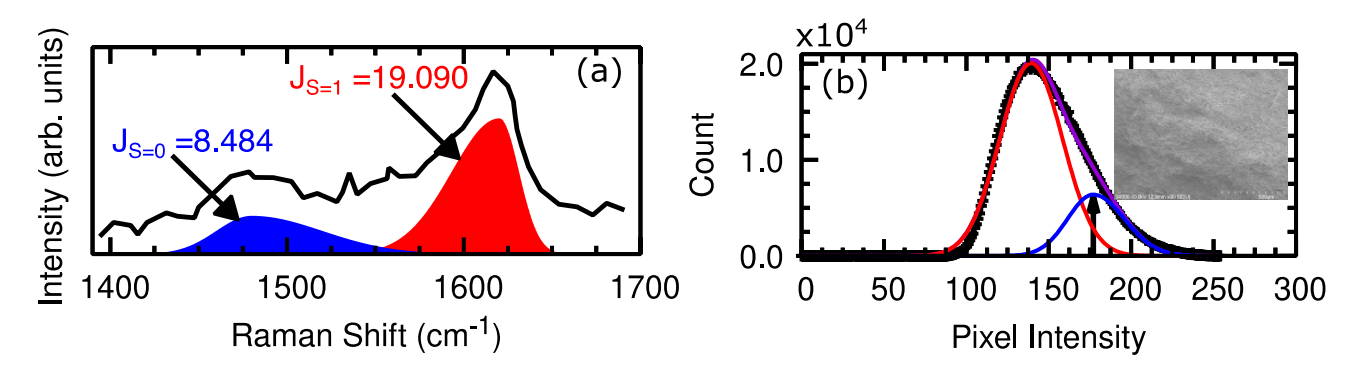


Figure 1. (a) Example S^2 analysis method using a Raman spectrum of a PANI fiber. The red area corresponds to $J_{S=1}$ and the blue area corresponds to $J_{S=0}$. Using the values for $J_{S=1}$ and $J_{S=0}$ indicated on the plot and Eq. 1, the measured S^2 value from the spectrum is 0.6923. The Raman spectrum for the PANI sample was obtained from reference [17]. (b) Example of the S^2 analysis method for SEM images of PCL fibers. The plot shows the pixel intensity histogram for the inset SEM image along with the fitted curves for intensities associated with the ordered (blue) and disordered (red) structure components, along with the overall resulting fit (purple). The arrow indicates the resulting threshold value of 177. To determine S^2 , the number of pixels with intensities at or above the threshold value are summed (176424) and then divided by the total number of pixels (1228800) in the image to obtain $S^2 = 0.1436$.

Results and Discussion

Systems that undergo any order-to-disorder transition follow the theory of second-order Landau phase transitions [18]. If only the temperature is varied, then the order parameter of the system should linearly decrease to zero as the temperature increases to the critical temperature of the system. In the case of the structural order parameter *S*, the variation with temperature is given by

$$S^2 = \frac{\alpha_0}{\beta} T_c - \frac{\alpha_0}{\beta} T \tag{2}$$

where α_0 and β are material-dependent constants that are always positive, and T_c is the critical temperature below which S=0. Thus, linear behavior of S with temperature can be used to establish that a system has the potential to be characterized by varying degrees of structural disorder. We have previously demonstrated this is the case for polypropylene based on an experimentally-observed linear relationship between S^2 and temperature. As can be seen in Figure 2, both PANI and PVDF polymers also exhibit a linear relationship between S^2 and temperature, indicative of an order-to-disorder transition.

For both PANI and PVDF, the S^2 value was extracted from Raman spectra acquired at different temperatures. In the case of PANI fibers, the peak at ~1475 cm⁻¹ (assigned to stretching of the double carbon nitrogen bonds) is associated with the disordered structure, and the peak at ~1620 cm⁻¹ (due to carbon-to-carbon bond stretching) is associated with the ordered structure. In the case of PVDF fibers, the peak at ~810 cm⁻¹ is associated disordered structure, and the peak at ~840 cm⁻¹ is associated with the ordered structure. For both polymers, the disordered and ordered structure peaks were identified by observing the evolution of the spectra with temperature. The area under the disordered structure peaks vary as $(1 - S^2)$ and the area under the peaks associated with the ordered structure vary as $S^2[15]$, [16]; thus, with increasing temperature (and thus decreasing S by Equation 2) disordered structure peaks increase in intensity, whereas ordered structure peaks decrease in intensity. This can be seen in Figure 2a and b (c and d) for PANI (PVDF) where the area under the peak at 1475 cm⁻¹ (810 cm⁻¹) increases with temperature, whereas the area under the peak at 1620 cm⁻¹ (840 cm⁻¹) decreases. Figure 2e shows the temperature behavior of S^2 for PANI and PVDF samples; in both cases, the linear relationship

expected for a system undergoing an order to disorder transition is observed, indicating that these polymer systems can experience varying degrees of disorder within their structures.

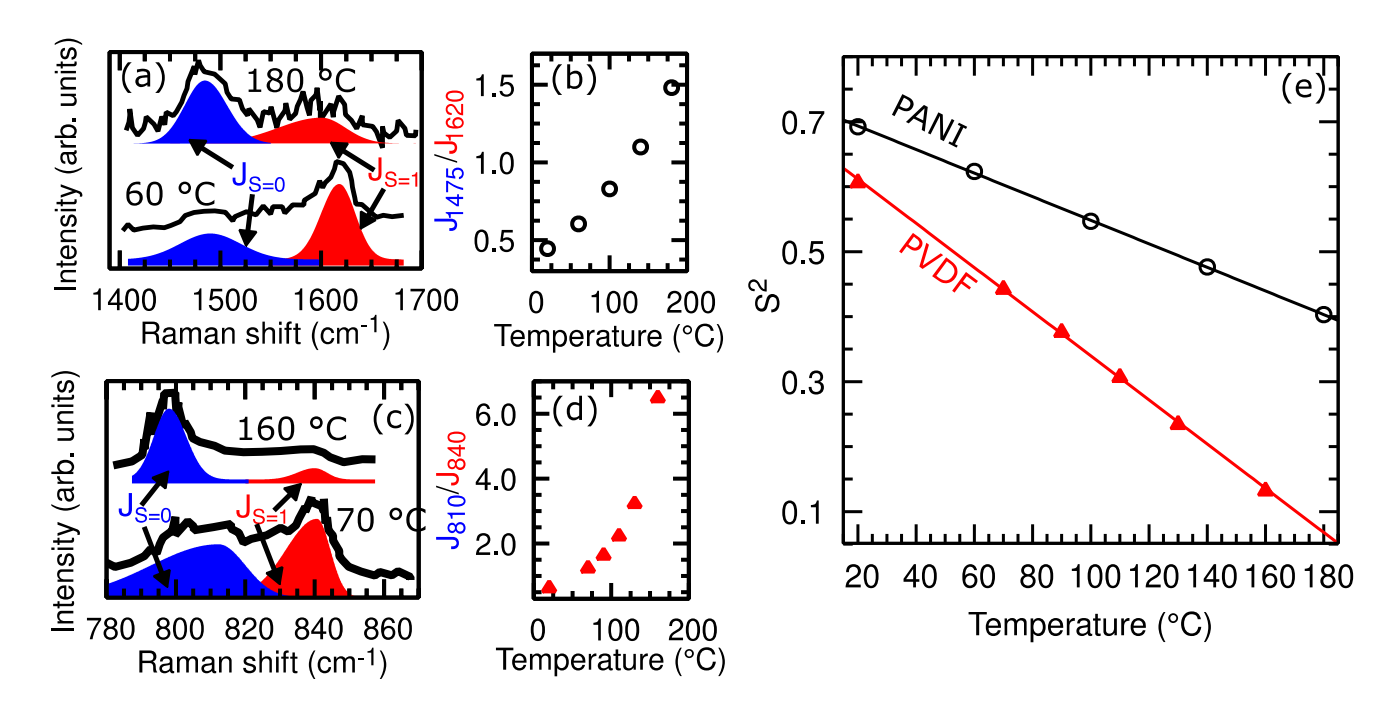


Figure 2. (a) Raman spectra of a PANI sample at 180 °C and 60 °C. (b) The ratio of the area under the peak at 1475 cm⁻¹ (J_{1475}) to the area under the peak at 1620 cm⁻¹ (J_{1620}) as a function of temperature. (c) Raman spectra of a PVDF sample at 160 °C and 60 °C. (d) The ratio of the area under the peak at 810 cm⁻¹ (J_{180}) to the area under the peak at 1620 cm⁻¹ (J_{840}) as a function of temperature. For (a) and (c) the blue curves represent the Raman peaks associated with the disordered phase and the red curves represent the peaks associated with the ordered phase of the polymers. (e) S^2 as a function of temperature for PANI and PVDF polymer samples. The S^2 values were obtained from Raman spectra from reference [17] for the PANI sample and from reference [19] for PVDF.

It can be shown that system-level properties that are dominated by pair-wise or single interactions have a linear dependence on S^2 [13], [14]. Specifically,

$$P(x,S) = S^{2}[P(0.5,1) - P(x,0)] + P(x,0)$$
(3)

where P(x,S) is the system level property at a given composition x and value of S. In the case of polymer systems, we have shown that this relationship applies to the filtration efficiency of masks made from polypropylene, polypropylene/polyethylene bicomponent spunbond (PP/PE-BCS) or polybenzimidazole (PBI) [10]. We extend this now to the electrical properties of PANI fibers.

Experimental data for PANI samples were taken from the literature and the corresponding S^2 values determined from SEM images. As seen in Figure 3a, there is a clear relationship between the band gap of PANI samples and the value of S^2 , as predicted by Equation 3. Thus, increasing disorder with the structure of PANI polymers (understood in the context of tacticity [10]) leads to an increase in the band gap of PANI. Interestingly, the specific capacitance of PANI polymers shows the opposite dependence on disorder compared to the band gap, as shown in Figure 3b; increasing disorder in the polymer leads to a lower specific capacitance.

Once the relationships illustrated in Figure 3 are determined, we are then presented with the means to further tune the band gap and specific capacitance of PANI polymers by controlling the degree of disorder characterizing the samples. For example, extrapolation of the experimentally-determined points in Figure 3a indicates that band gaps in the range of 0.74 eV for a perfectly ordered polymer to 4.07 eV for completely disordered sample are achievable. Likewise, Figure 3b indicates that specific capacitance in the range of 215 F/g for a completely disordered sample to 645 F/g for an ordered sample are achievable for PANI polymers.

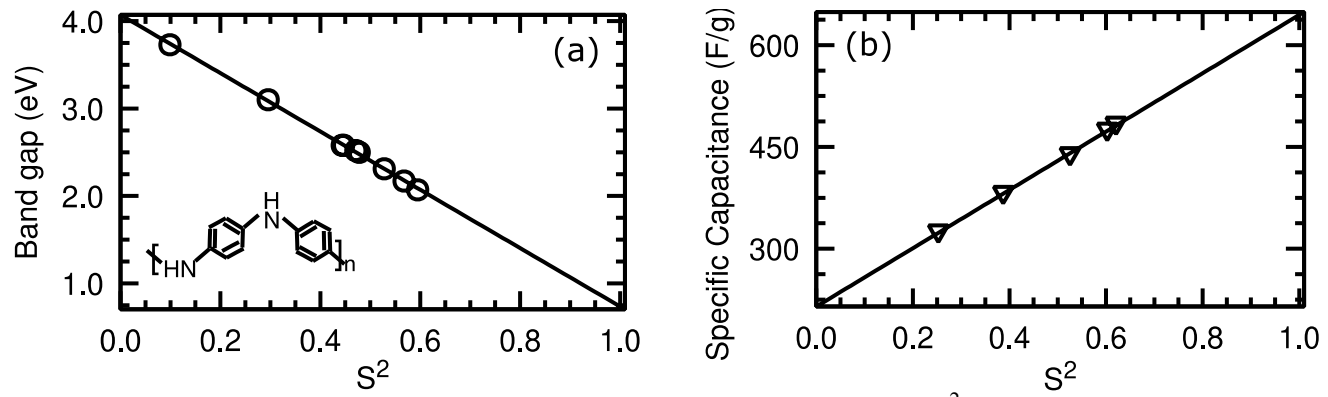


Figure 3. (a) The experimental relationship between the band gap and S^2 for PANI polymer fibers. Inset is a possible molecular structure for the S=1 state for PANI. (b) The experimental relationship between the specific capacitance of PANI samples and S^2 . S^2 was determined from SEM images for all points. Data was analyzed from references [20]–[24] for (a) and from reference [25] for (b).

Unsurprisingly, disorder can also influence the structural properties of polymers. To investigate this relationship, the S^2 value of samples of PCL and PANI-PCL grown by electro-spinning were measured via SEM images and their Young's modulus measured using stress-strain curves. Figure 4a shows the experimental data for Young's modulus of PCL as a function of S^2 . The trend shows that increasing structural disorder in the PCL polymers results in a linear increase in the Young's modulus of the sample. It is interesting to note that the larger morphology observed (designated 'aligned,' 'honeycomb' or 'random' based on appearance) in these samples appears to correspond to a compositional change in the disorder modeling system. The Young's modulus of PANI-PCL samples also increases with increasing disorder, as seen in Figure 4b. The variation in disorder for the PANI-PCL samples can be attributed to varying the applied voltage during synthesis; increasing the applied voltage leads to an increase in the degree of disorder in the samples, as well as a change in their composition. Additionally, we analyzed the Young's modulus as a function of disorder for PVDF data in the literature [26], [27]. Interestingly, PVDF shows an opposite relationship between the Young's modulus and disorder than PCL and PANI-PCL, namely that increasing disorder leads to a linearly decreasing value of Young's modulus. For all three material systems, however, there exists a linear relationship between S^2 and the Young's modulus value, as predicted by Equation 3. We should also note that extrapolation of the Young's modulus data in Figure 4 suggests that under certain circumstances, it may be possible to tune the degree of disorder to obtain a negative value of Young's modulus in a sample—without the need for metamaterial strategies [28]–[30], and in a fashion similar to what was observed for the band gap energy of compound semiconductors [14].

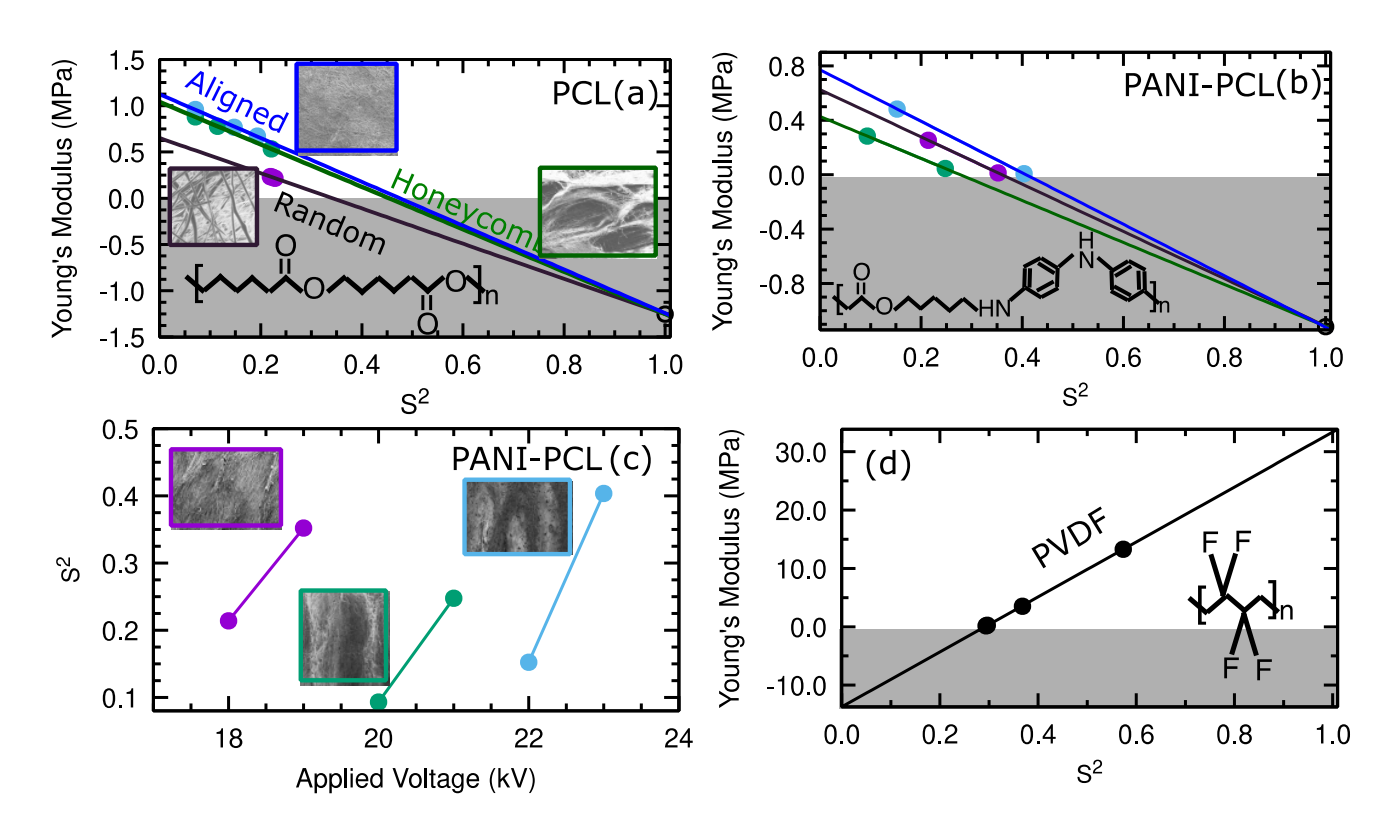


Figure 4. Experimentally determined relationship between Young's Modulus and S^2 for (a) PCL fibers (b) PANI-PCL fibers. (c) S^2 as a function of the applied voltage during the electro-spinning process for PANI-PCL fibers. (d) Experimentally determined relationship between Young's Modulus and S^2 for PVDF fibers. S^2 was measured from SEM images for all data points. The data analyzed for (d) was extracted from references [26], [27]. Filled symbols represent experimental data points. The open symbol at $S^2 = 1$ denotes the extrapolated endpoint. *Insets*: (a) SEM images of each different PCL morphology and a possible molecular structure of S=1 PCL; (b) A possible molecular structure of S=1 PANI-PCL; (c) SEM images of samples at each of the different PANI-PCL composition values, and (d) a possible molecular structure of S=1 PVDF.

Conclusion

Quantifying the degree of structural disorder in polymers provides a pathway to uncover relationships between disorder and system-level properties of polymers. Electrical properties of polymers, such as the band gap and specific capacitance, and structural properties, such as Young's modulus, can be tuned over a wide range of values for a given polymer system by controlling the degree of order. This degree of order can be tuned through growth conditions or by post heat treatment of samples. In addition, extrapolation of experimental data suggests that in some instances it may be possible to obtain a negative Young's modulus by tuning disorder, potentially obviating the need for metamaterial strategies.

Data Availability

The datasets generated during and/or analyzed during the current study are available from the corresponding author on reasonable request.

Acknowledgements

This work was performed with partial support from the National Science Foundation (DMR-2003581, S.D and R.M.) and Western Michigan University. Analysis was performed using hardware received through the NVIDIA Academic Hardware grant program (R.M.). S.H would like to acknowledge

supported by the Portage Health Foundation (PHF) Graduate Assistantship and the Michigan Tech Finishing Fellowship.

Competing Interests

R.M. and S.D. have a pending patent application on tuning polymer properties through disorder.

References

- [1] M. Beygisangchin, S. Abdul Rashid, S. Shafie, A. R. Sadrolhosseini, and H. N. Lim, "Preparations, Properties, and Applications of Polyaniline and Polyaniline Thin Films—A Review," *Polymers*, vol. 13, no. 12, Art. no. 12, Jan. 2021, doi: 10.3390/polym13122003.
- [2] Y. Chen *et al.*, "Polyaniline electrospinning composite fibers for orthotopic photothermal treatment of tumors in vivo," *New J. Chem.*, vol. 39, no. 6, pp. 4987–4993, Jun. 2015, doi: 10.1039/C5NJ00327J.
- [3] M.-C. Chen, Y.-C. Sun, and Y.-H. Chen, "Electrically conductive nanofibers with highly oriented structures and their potential application in skeletal muscle tissue engineering," *Acta Biomater.*, vol. 9, no. 3, pp. 5562–5572, Mar. 2013, doi: 10.1016/j.actbio.2012.10.024.
- [4] F. F. F. Garrudo *et al.*, "Polyaniline-polycaprolactone blended nanofibers for neural cell culture," *Eur. Polym. J.*, vol. 117, pp. 28–37, Aug. 2019, doi: 10.1016/j.eurpolymj.2019.04.048.
- [5] S. Nagam Hanumantharao, C. Que, and S. Rao, "Self-assembly of 3D nanostructures in electrospun polycaprolactone-polyaniline fibers and their application as scaffolds for tissue engineering," *Materialia*, vol. 6, p. 100296, Jun. 2019, doi: 10.1016/j.mtla.2019.100296.
- [6] S. H. Ku, S. H. Lee, and C. B. Park, "Synergic effects of nanofiber alignment and electroactivity on myoblast differentiation," *Biomaterials*, vol. 33, no. 26, pp. 6098–6104, Sep. 2012, doi: 10.1016/j.biomaterials.2012.05.018.
- [7] A. Sanyal and S. Sinha-Ray, "Ultrafine PVDF Nanofibers for Filtration of Air-Borne Particulate Matters: A Comprehensive Review," *Polymers*, vol. 13, no. 11, Art. no. 11, Jan. 2021, doi: 10.3390/polym13111864.
- [8] R. Noriega *et al.*, "A general relationship between disorder, aggregation and charge transport in conjugated polymers," *Nat. Mater.*, vol. 12, no. 11, Art. no. 11, Nov. 2013, doi: 10.1038/nmat3722.
- [9] D. Golodnitsky, E. Strauss, E. Peled, and S. Greenbaum, "Review—On Order and Disorder in Polymer Electrolytes," *J. Electrochem. Soc.*, vol. 162, no. 14, p. A2551, Oct. 2015, doi: 10.1149/2.0161514jes.
- [10] R. A. Makin, K. R. York, A. S. Messecar, and S. M. Durbin, "Quantitative Disorder Analysis and Particle Removal Efficiency of Polypropylene-Based Masks," *MRS Adv.*, vol. 5, no. 56, pp. 2853–2861, ed 2020, doi: 10.1557/adv.2020.346.
- [11] E. J. Williams and W. L. Bragg, "The effect of thermal agitation on atomic arrangement in alloys-III," *Proc. R. Soc. Lond. Ser. Math. Phys. Sci.*, vol. 152, no. 875, pp. 231–252, 1935, doi: 10.1098/rspa.1935.0188.
- [12] S. N. Hanumantharao, C. A. Que, B. J. Vogl, and S. Rao, "Engineered Three-Dimensional Scaffolds Modulating Fate of Breast Cancer Cells Using Stiffness and Morphology Related Cell Adhesion," *IEEE Open J. Eng. Med. Biol.*, vol. 1, pp. 41–48, 2020, doi: 10.1109/OJEMB.2020.2965084.
- [13] R. A. Makin *et al.*, "Alloy-Free Band Gap Tuning across the Visible Spectrum," *Phys. Rev. Lett.*, vol. 122, no. 25, p. 256403, Jun. 2019, doi: 10.1103/PhysRevLett.122.256403.
- [14] R. A. Makin, K. York, S. M. Durbin, and R. J. Reeves, "Revisiting semiconductor band gaps through structural motifs: An Ising model perspective," *Phys. Rev. B*, vol. 102, no. 11, p. 115202, Sep. 2020, doi: 10.1103/PhysRevB.102.115202.

- [15] J. M. Loveluck and J. B. Sokoloff, "Theory of the optical properties of phonon systems with disordered force constants, with application to NH4Cl," *J. Phys. Chem. Solids*, vol. 34, no. 5, pp. 869–884, May 1973, doi: 10.1016/S0022-3697(73)80089-7.
- [16] R. A. Makin *et al.*, "Alloy-Free Band Gap Tuning across the Visible Spectrum," *Phys Rev Lett*, vol. 122, no. 25, p. 256403, Jun. 2019, doi: 10.1103/PhysRevLett.122.256403.
- [17] J. Zhang, C. Liu, and G. Shi, "Raman spectroscopic study on the structural changes of polyaniline during heating and cooling processes," *J. Appl. Polym. Sci.*, vol. 96, no. 3, Feb. 2005, doi: https://doi.org/10.1002/app.21520.
- [18] D. Chowdhury and D. Stauffer, "Mean-Field Theory III: Landau Formulation," in *Principles of Equilibrium Statistical Mechanics*, John Wiley & Sons, Ltd, 2000, pp. 432–469. doi: https://doi.org/10.1002/3527603158.ch12.
- [19] S. Satapathy, S. Pawar, P. K. Gupta, and K. B. R. Varma, "Effect of annealing on phase transition in poly(vinylidene fluoride) films prepared using polar solvent," *Bull. Mater. Sci.*, vol. 34, no. 4, p. 727, Oct. 2011, doi: 10.1007/s12034-011-0187-0.
- [20] H. Goktas, Z. Demircioglu, K. Sel, T. Gunes, and I. Kaya, "The optical properties of plasma polymerized polyaniline thin films," *Thin Solid Films*, vol. 548, pp. 81–85, Dec. 2013, doi: 10.1016/j.tsf.2013.09.013.
- [21] O. Belgherbi, L. Seid, D. Lakhdari, D. Chouder, M. S. Akhtar, and M. A. Saeed, "Optical and Morphological Properties of Electropolymerized Semiconductor Polyaniline Thin Films: Effect of Thickness," *J. Electron. Mater.*, vol. 50, no. 7, pp. 3876–3884, Jul. 2021, doi: 10.1007/s11664-021-08896-7.
- [22] V. K T and S.L.Belagali, "Characterization of Polyaniline for Optical and Electrical Properties," *IOSR J. Appl. Chem.*, vol. 8, no. I, Jan. 2015, doi: 10.9790/5736-0801025356.
- [23] S. Bhadra, S. Chattopadhyay, N. K. Singha, and D. Khastgir, "Improvement of conductivity of electrochemically synthesized polyaniline," *J. Appl. Polym. Sci.*, vol. 108, no. 1, pp. 57–64, 2008, doi: 10.1002/app.26926.
- [24] G. B. V. S. Lakshmi, A. Dhillon, A. M. Siddiqui, M. Zulfequar, and D. K. Avasthi, "RF-plasma polymerization and characterization of polyaniline," *Eur. Polym. J.*, vol. 45, no. 10, pp. 2873–2877, Oct. 2009, doi: 10.1016/j.eurpolymj.2009.06.027.
- [25] W. Shao, R. Jamal, F. Xu, A. Ubul, and T. Abdiryim, "The Effect of a Small Amount of Water on the Structure and Electrochemical Properties of Solid-State Synthesized Polyaniline," *Materials*, vol. 5, no. 10, Art. no. 10, Oct. 2012, doi: 10.3390/ma5101811.
- [26] P. K. Szewczyk, D. P. Ura, and U. Stachewicz, "Humidity Controlled Mechanical Properties of Electrospun Polyvinylidene Fluoride (PVDF) Fibers," *Fibers*, vol. 8, no. 10, Art. no. 10, Oct. 2020, doi: 10.3390/fib8100065.
- [27] R. L. Hadimani *et al.*, "Continuous production of piezoelectric PVDF fibre for e-textile applications," *Smart Mater. Struct.*, vol. 22, no. 7, p. 075017, Jun. 2013, doi: 10.1088/0964-1726/22/7/075017.
- [28] J.-H. Lee, J. P. Singer, and E. L. Thomas, "Micro-/Nanostructured Mechanical Metamaterials," *Adv. Mater.*, vol. 24, no. 36, pp. 4782–4810, 2012, doi: 10.1002/adma.201201644.
- [29] T.-C. Lim, Mechanics of Metamaterials with Negative Parameters. Springer Nature, 2020.
- [30] Z. Hou and B. M. Assouar, "Tunable solid acoustic metamaterial with negative elastic modulus," *Appl. Phys. Lett.*, vol. 106, no. 25, p. 251901, Jun. 2015, doi: 10.1063/1.4922873.